

Theoretical and experimental study of space charge in intense ion beams

A. J. T. Holmes

Culham Laboratory, Abingdon-Oxon OX14 3DB, England

(Received 15 May 1978)

The highly collimated beams of energetic neutral atoms used in controlled thermonuclear fusion research (CTR) require the virtual elimination of space-charge forces in the primary ion beam in order to minimize the angular divergence. A model is presented which describes the behavior of an intense ion beam passing through a gas cell. This theory is used to derive the space-charge field produced by such a beam and shows how its effect can be minimized. This model agrees well with experimental measurements and enables emittance-dominated beams of very high brightness to be obtained which could find applications in fields other than CTR.

I. INTRODUCTION

The injection of beams of energetic neutral atoms is one of the major methods of auxiliary heating presently in use in the field of controlled thermonuclear research (Cordey^{1,2} and Kulsrad and Jassby³). These beams are formed by electron capture of a positive-ion beam passing through a gas cell. In order to maximize the power transfer from the ion source to the fusion plasma, and also to minimize the flux of thermal gas, the ion beam and therefore the resulting neutral beam should be highly collimated.

Part of the neutral-beam-injection development program at the Culham Laboratory has been specifically aimed towards elucidating the fundamental limits to the divergence of ion beams passing through gas at low pressure. It has been found that residual space-charge expansion of a nominally space-charge-neutralized beam was one of the major processes responsible for divergence angles of the order of 1° observed in previous work. A model is presented below that describes the processes involved in the space-charge neutralization of ion beams and, using the predictions of this model, ion beams have been generated in which the divergence due to residual space-charge expansion is insignificant compared with that due to the finite temperature of the beam ions. Although developed for fusion research, these low divergence beams ($\sim 0.2^\circ$) which have a normalized brightness of 3×10^{12} mA cm⁻² sr⁻¹, may find other applications.

II. PHYSICAL PROCESSES

The model considers a nonrelativistic ion beam, remote from any conducting walls, passing through a gas at low pressure. Electrons, produced by ionization, are trapped within the beam by its own space charge, resulting in a decrease of the ef-

fective beam perveance, and hence space-charge expansion, to a value that is considerably less than that of the unneutralized beam. The energy and particle balance of this system are explored in some detail as functions of the various physical parameters of the primary beam and in particular as a function of the ambient gas pressure. The use of Poisson's equation enables a self-consistent description of the beam plasma to be made, including the radial dependence of the potential and particle densities within the beam. It is the radial electric field of the beam plasma that is responsible for the space charge expansion of the beam.

In previous theoretical treatments of space-charge neutralization of ion beams, either the continuity or the energy balance equation has been neglected or Poisson's equation has been replaced by the plasma neutrality equation. In the model described by Gabovich *et al.*,⁴ electron continuity is neglected and plasma neutrality for a uniform-density beam is assumed, thus losing all spatial information. An alternative model developed by Hamilton⁵ neglects the effects of the slow ions formed by ionization and also uses the plasma neutrality condition. The neutralization of electron beams, which is very similar, is discussed by Dunn and Self,⁶ who have solved Poisson's equation by giving an analytic spatial distribution for the electrons and slow ions in a uniform beam but they do not consider the energy balance of the plasma, which controls the electron temperature. Green⁷ has extended Dunn and Self's model to cover ion beams but does not consider energy balance.

The model presented here uses the continuity equation to describe the slow ion and electron densities and the electron temperature is determined by considering the overall energy balance of the beam plasma system. The potential well can then be found by using Poisson's equation,

thus completing the description of the beam plasma. Unfortunately these equations are complex and involve four nonlinear differential equations that would require very sophisticated numerical techniques for solution. A slightly simpler approach is adopted here, which creates an approximate intermediate solution for the potential that allows the four differential equations to be reduced to a single nonlinear equation that still requires a numerical solution, but is considerably simpler to obtain. This new solution replaces the intermediate solution and also provides a comparison to ensure that the intermediate solution is a good approximation. An even simpler technique of solution is also presented that replaces Poisson's equation by plasma neutrality and discards the spatial-distribution functions. This method obtains approximate analytic expressions describing the axial potential and charge densities as functions of the main beam parameters and is useful in understanding the general scaling laws of the beam plasma.

The continuity equation is applied separately to each species of particle. The slow-ion flux is determined by an equilibrium between the rate of creation by ionization and charge exchanging collisions and the rate of expulsion by the radial electric field. The electrons, however, are trapped by this electric field and can only escape by diffusion in velocity space via electron-electron collisions until they reach the tail of the Maxwellian distribution and escape.

The electrons formed by ionization extract energy from the primary ion beam by Coulomb collisions. The electron heating by the beam is controlled by the detailed shape of the electron distribution at low velocities, which is modified by the presence of newly created electrons. The Fokker-Planck equation is used to determine the electron distribution function that is treated as a perturbed Maxwellian distribution. The heated electrons control the magnitude of the potential well and hence determine the energy removed by the escaping slow ions as they are accelerated radially outwards. This energy is equal to the average binding energy of electrons trapped in the well and if these electrons are to escape, they must absorb an equivalent energy from the primary ion beam.

Green⁷ has pointed out that the slow ions formed by charge exchange are not involved in the above energy balance. The energy for this process comes directly from the beam ions that are all decelerated by the space-charge potential shortly after they have left the emitter, which is assumed to be at the wall potential. In the absence of charge exchange, the beam ions are reaccelerated

to their full energy when they leave the space-charge well at the distant target (also at the wall potential) and there is no net energy transfer. If a beam ion is converted to a fast neutral within the well, however, it cannot be reaccelerated and the energy lost by the beam ion entering the space charge well is removed by the resulting slow ion when it is expelled radially. Hence this energy transfer is independent of the beam parameters and does not affect the electron temperature.

III. CONTINUITY EQUATION

The densities of the slow ions and electrons can be derived from the solution of the continuity equation in terms of the other plasma parameters. The general form of the equation is

$$\frac{\partial n_j}{\partial t} + \nabla \cdot \vec{F}_j = 0, \quad (1)$$

where $\partial n_j / \partial t$ is the creation (or loss) rate of particle j and F_j is the particle flux. This flux describes the motion of each species, which in the case of slow ions is free fall under the influence of the electric field. The electrons, however, are assumed to be born with essentially zero velocity and hence they are electrostatically contained by the fast-ion space charge. In this case the escaping electron flux is governed by their diffusion in velocity space. These fluxes and their effect on the particle densities are discussed in Secs. III A and III B.

It is assumed that the beam ions alone are responsible for the creation of slow ions and electrons. The secondary-electron energy distribution lacks a high-energy tail (see Sec. III B and Fig. 1) and hence the production rate of ion-electron pairs by these electrons is very much less than that of the beam for the experimental situation discussed here (i.e., $10^{-6} < p < 10^{-2}$ Torr).

A. Ions

It is now appropriate to use the integral form of Eq. (1), obtained by the use of Green's theorem, which gives

$$\int_V \frac{\partial n_j}{\partial t} dV = \int_S \vec{F}_j \cdot d\vec{S}.$$

As the beam has cylindrical symmetry, the ion flux is purely radial and they can only escape at infinity, there being no sinks for ions at finite radius (the conducting walls are assumed to be at infinity). Hence for a creation rate dn_i/dt in an element of volume $2\pi\rho d\rho dz$ and where these ions move to a surface at r , the above equation

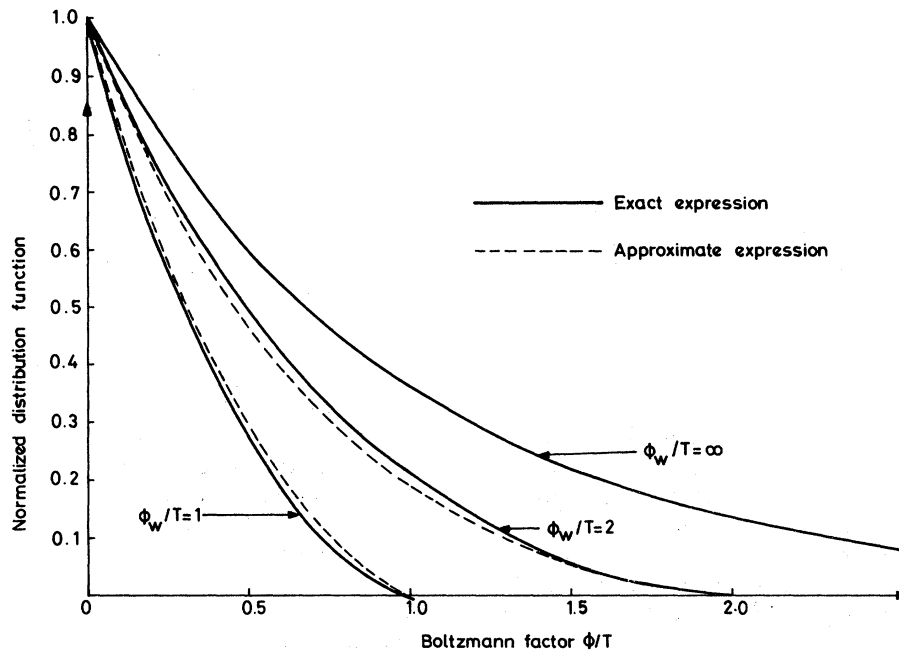


FIG. 1. Dependence of the electron distribution function on the potential well depth ϕ_w .

transforms to

$$\frac{\partial n_i}{\partial t} 2\pi\rho d\rho dz = 2\pi r dz F_i = 2\pi r dz v(\rho, r) dn_i(r),$$

where $v(\rho, r)$ is the velocity at r of those ions produced at ρ and $dn_i(r)$ is the contribution to the density of the ions at r . Integration gives

$$n_i(r) = \frac{1}{r} \int_0^r \frac{\partial n_i}{\partial t} \frac{\rho d\rho}{v(\rho, r)}. \quad (2)$$

The slow ions are created by ionization and charge exchange and move freely under the influence of the electric field. (Scattering is unimportant as the time they spend within the beam is typically the order of $1 \mu\text{sec}$ and is much less than the Coulomb interaction time for pressures less than 0.1 Torr .) Hence

$$n_i(r) = \frac{1}{r} \int_0^r \frac{n_b \sigma v_b n \rho d\rho}{(2e/m_i)^{1/2} [-\phi(r) + \phi(\rho)]^{1/2}}, \quad (3)$$

where n_b is the beam density at ρ , v_b is the beam velocity, n is the gas density, and σ is the sum of the ionization and charge-exchange cross sections.

It is shown in Appendix A that the only finite solution for n_i at small values of r is

$$\lim_{r \rightarrow 0} n_i(r) = n_{i0} = n_{b0} r_0 \sigma n v_b m_i^{1/2} / (2e\phi_0)^{1/2}, \quad (4)$$

where ϕ_0 is defined as the first coefficient of the series

$$-\phi(r) = \phi_0 \frac{r^2}{r_0^2} + \phi_1 \frac{r^3}{r_0^3} + \dots$$

Hence the potential well has a parabolic form close to the beam axis. At larger radii where $n_b \neq n_{b0}$, the potential need no longer remain parabolic and n_i can be found by numerical integration of Eq. (2).

B. Electrons

Low-energy electrons created within the beam are trapped by the space charge of the fast ions. To the lowest order, electron-electron collisions lead to the development of a Maxwellian distribution, characterised by a temperature T (eV); diffusion in velocity space allows the electrons which would have populated the high-energy tail of the distribution to escape. Hence the electron particle balance is governed by the rate of electron production by ionization and the rate of escape, which is determined by the depth of the potential well, and the electron temperature and density. The corresponding energy balance required to maintain this temperature is discussed in Sec. IV.

Clearly the lifetime of an individual electron depends upon its position in the well; an electron created near the beam axis, and therefore at the bottom of the well, must diffuse much further in velocity space prior to being able to escape than one created near the beam edge where

the well is relatively shallow. The electron density in velocity space can be obtained in terms of the source function, electron temperature, and potential distribution. The electron density in real space can then be found by recalling that the coordinates of real and velocity space are coupled via the potential well.

Spitzer⁸ has shown that the time for a subgroup of electrons to increase their velocity dispersion by an amount v in the directions perpendicular and parallel to their original motion is

$$\tau_{\perp} = v^2 / \langle (\omega_{\perp})^2 \rangle, \quad \tau_{\parallel} = v^2 / \langle (\omega_{\parallel})^2 \rangle,$$

where $\langle (\omega_{\parallel})^2 \rangle$ and $\langle (\omega_{\perp})^2 \rangle$ are the dispersion coefficients in these directions. For a Maxwellian electron distribution of density $n_e(r)$, and using Spitzer's notation, these are

$$\langle (\omega_{\parallel})^2 \rangle = \frac{e^4 n_e \ln \Lambda}{2\pi \epsilon_0^2 m_e^2} \frac{G(l_f \omega)}{\omega} = A_d \frac{G(l_f \omega)}{\omega},$$

$$\langle (\omega_{\perp})^2 \rangle = \frac{A_d}{\omega} [\operatorname{erf}(l_f \omega) - G(l_f \omega)],$$

where ω is the electron test-particle velocity. If, as is the case here, the electron test particles in the subgroup are identical with the main distribution, then ωl_f equals $\sqrt{1.5}$.

Since the initial velocities in the subgroup are randomly orientated, neither the perpendicular nor parallel directions have any special significance and the two diffusion times may be combined to give a net time

$$\tau = (1/\tau_{\perp} + 1/\tau_{\parallel})^{-1} = v^2 [\langle (\omega_{\perp})^2 \rangle + \langle (\omega_{\parallel})^2 \rangle] \\ = v^2 \omega / A_d \operatorname{erf}(\sqrt{1.5}).$$

The velocity dispersion coefficient may be considered as a diffusion coefficient in velocity space with a magnitude

$$D_v = \frac{\operatorname{erf}(\sqrt{1.5}) A_d}{\omega} = \frac{0.97 e^4 n_e \ln \Lambda}{2\pi \epsilon_0^2 m_e^2 \omega} \\ = C n_e.$$

This diffusion coefficient scales differently from the neutral-gas diffusion coefficient as it is proportional to the particle density.

The potential well that surrounds the beam relates the velocity of the electrons to their radius of oscillation in the well. Hence diffusion in velocity space is equivalent to radial diffusion in real space and the source-distribution function in real space causes the electrons to have an analogous source function in velocity space. As it has been assumed that the velocity distribution is Maxwellian throughout the potential well, it is not necessary to use the full distribution function f for the electrons. Instead, a simplified function

n_v that describes the number of electrons whose velocity lies in the range v to $v+dv$ relative to a given origin can be used. This velocity can be directly related to the binding potential and containment time since the electrons spend most of their time at the turning points of the oscillation and they also conserve their random kinetic energy.

The primary ion beam is assumed to be axially and azimuthally uniform with no spatial diffusion in these directions, hence

$$n_v = n_e \left| \frac{2\pi r dr}{2\pi v_r dv_r} \right|$$

where v_r represents the velocity increment to escape. The diffusion equation can be represented by

$$\nabla(D_v \nabla n_v) = -\frac{dn_v}{dt},$$

which in cylindrical geometry becomes

$$\frac{1}{v_r} \frac{d}{dv_r} \left(v_r D_v \frac{dn_v}{dv_r} \right) = -n v_b \sigma_i v_b \frac{2\pi r dr}{2\pi v_r dv_r}. \quad (5)$$

Before further progress can be made, the beam profile must be known. The beam profile is assumed, *a priori*, to have a Gaussian shape, so that

$$n_b = n_{b0} e^{-r^2/r_0^2}. \quad (6)$$

Hence the first integration of Eq. (5) can be made giving

$$v_r D_v \frac{dn_v}{dv_r} = \frac{n n_{b0} \sigma_i v_b r_0^2}{2} e^{-r^2/r_0^2} + A. \quad (7)$$

In order to integrate further, the transform relation between v_r and r must be determined.

There are two natural coordinate systems in velocity space, namely, one where the velocity is related to the potential energy associated with the radius of oscillation so that $v=0$ when $r=0$, and the other where the velocity is related to the binding energy so that $v=0$ when $r=\infty$. The latter coordinate system has a better physical basis as it is directly connected to the confinement time and hence it will be adopted, giving

$$v_r^2 = \frac{2e\Delta\phi}{m_e} = \frac{2e}{m_e} [\phi_w + \phi(r)],$$

where ϕ now represents the velocity required to overcome the binding energy when the electron is at its turning points (where it is most of the time).

A first approximation to the potential distribution with respect to radius may be made by assuming it also to be Gaussian but with a different radius r_0/β , so that

$$\phi(r) = -\phi_w (1 - e^{-(\beta r/r_0)^2}). \quad (8)$$

This approximation is strongly supported by experiment and also by the full numerical solution of Poissons equation that replaces Eq. (8). Hence

$$v_r^2 = (2e\phi_w/m_e)e^{-(\beta r/r_0)^2} = v_m^2 e^{-(\beta r/r_0)^2}.$$

The other coordinate system for v gives an identical electron distribution, but breaks down at large values of r because of the approximation assumed for ϕ .

Returning to Eq. (7), it can be seen that A must be zero and if the dependence of D_p on n_e is included, then on integration the equation becomes

$$Cn_v^2 = \frac{nm_{b0}\alpha_1 v_b r_0^4}{\beta^2(2/\beta^2 - 2)} \left(\frac{v^2}{v_m^2}\right)^{1/\beta^2} \frac{1}{v^2} + B.$$

When the transform is applied in reverse, the electron density in real space may be obtained as

$$Cn_e^2 = \frac{nm_{b0}\sigma_1 v_b \beta^2 v_m^2}{(2/\beta^2 - 2)} e^{-r^2/r_0^2} e^{-(\beta r/r_0)^2} + \frac{B\beta^4}{r_0^4} v_m^2 e^{-(\beta r/r_0)^2}.$$

However, the electron density is expected to decrease more rapidly than the potential; hence the numerical constant of integration B must be zero. The final solution for the electron density is

$$n_e = n_{e0} \left[\frac{(\frac{1}{4}\pi)^{1/2} \operatorname{erf}[\sqrt{(\phi_w + \phi)/T}] \exp(\phi + \phi_w)/T - \sqrt{(\phi + \phi_w)/T}}{(\frac{1}{4}\pi)^{1/2} \operatorname{erf}(\sqrt{\phi_w/T}) \exp\phi_w/T - \sqrt{\phi_w/T}} \right],$$

which is the truncated Maxwellian distribution of electrons in a well of finite depth.

Curves of n_e/n_{e0} are shown in Fig. 1 for several values of ϕ_w/T . A more tractable form of the above equation is obtained by numerical approximation to the above curves yielding

$$n_e = n_{e0} e^{(\phi/T)(\phi + \phi_w)/\phi_w}. \quad (10)$$

This is also used in the numerical analysis discussed in Sec. V.

It is clear that the distribution functions in Eqs. 9 and 10 must be made identical. This is achieved through the correct choice of β , which in turn involves the consideration of the energy balance of the system in order to determine T . However, knowledge of β is not required in the derivation of n_{e0} , the electron density on axis which can be obtained by inspection. If Eqs. (9) and (10) are combined, then

$$n_e = \left[\frac{4\beta^2}{0.97(2/\beta^2 - 2)} \frac{\pi\epsilon_0^2}{e^3 \ln\Lambda} \left(\frac{2eT}{m_e}\right)^{1/2} \times nm_{b0}\sigma_1 v_b m_e \phi_w \right]^{1/2} e^{\phi/T} \left(\frac{\phi_w + \phi}{\phi_w}\right). \quad (11)$$

$$n_e = \left[\frac{4\beta^2\pi}{0.97(2/\beta^2 - 2)} \frac{\epsilon_0^2}{e^3 \ln\Lambda} \times \left(\frac{2eT}{m_e}\right)^{1/2} nm_{b0}\sigma_1 v_b m_e \phi_w \right]^{1/2} \times \exp\left(-\frac{(1+\beta^2)r^2}{r_0^2}\right). \quad (9)$$

This solution is based on the assumption that the potential well has a Gaussian shape of radius r_0/β . Equation (9) above shows that the radius of the electron distribution is, as would be expected, intermediate between the beam radius r_0 and the potential radius and is $r_0[2/(1+\beta^2)]^{1/2}$.

It has been assumed that the trapped electrons have a Maxwellian distribution whereas in reality this distribution will be truncated at the velocity v_m , which causes the tail of the distribution to be lost. Virtually no electrons whose velocity exceeds v_m will be present as the electron transit time is shorter than 1% of the collision time. The truncated distribution function can be found using a method developed by Cordey,⁹ which gives

$$n_e = n_{e0} \int_{\epsilon=\phi}^{\epsilon=\phi_w} c^2 e^{-\epsilon/T} dc / \int_{\epsilon'=0}^{\epsilon'=\phi_w} c^2 e^{-\epsilon'/T} dc,$$

where $\epsilon = m_e c^2/2e - \phi$ and $\epsilon' = m_e c^2/2e$. This may be solved to give

The above expression shows that the value of β has only a small influence on the electron distribution.

IV. ELECTRON DISTRIBUTION AND ENERGY BALANCE

The energy balance of the beam plasma may be reduced to equating the energy loss arising from the escaping slow ions to the energy absorbed by the electrons arising from Coulomb collisions with the beam. The energy removed by slow ions produced by charge exchange does not enter into this energy balance because this energy comes from the electrostatic deceleration of the beam by its own potential well. In addition, the electrons cannot remove their kinetic energy eT from the beam as they escape when their energy just exceeds the binding potential.

The irreversible energy loss of the beam ions, when they pass through an electron gas, is critically dependent on the velocity distribution of the electrons and is maximum when the electron velocity is close to zero. In Sec. IIIB the electron velocity distribution was assumed to be Maxwellian with a cutoff at $v^2 = 2e\phi_w/m_e$. This cutoff

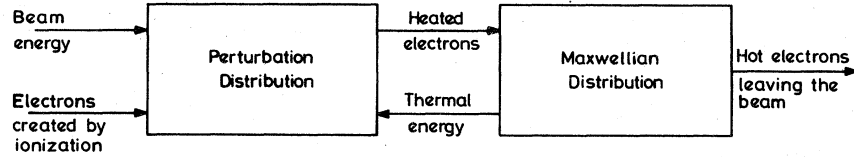


FIG. 2. Particle and energy transfer between the particle distributions. The total energy and particle content of each distribution is constant.

occurs at a velocity greater than v_b and hence will not affect the energy absorption. However it is possible to show (see Sec. IV C) that the energy absorbed by a true Maxwellian distribution of temperature T during the containment time is approximately an order of magnitude smaller than that required to escape. This arises from the high thermal velocity of the electrons that has been measured to be approximately twice the beam velocity.

Consequently another process is responsible for the energy absorption and it will be demonstrated below that the electron-distribution function at low velocities is considerably modified by the presence of newly created electrons that have low velocities and can hence act as good energy absorbers for the whose distribution. However, the number density of this group of electrons is low as they quickly thermalize with the main distribution.

The density and distribution function of these electrons can be evaluated from the Fokker-Planck equation. This function can then be used in the beam deceleration equation which determines the energy loss from the beam and hence equated to the energy removed by the slow ions.

A simple method showing the physics underlying this approach is shown in Fig. 2. The beam energy and newly created electrons enter the perturbed distribution. These electrons gain energy from the main distribution and also transfer energy and particles via the heated electrons which are absorbed into the main distribution. In this way the total energy and particle content of the perturbed distribution remains constant in time to give a steady state solution. Finally, the main Maxwellian distribution loses electrons which evaporate from the beam and also remove their binding energy from the beam thus maintaining the energy and particle content of this distribution.

A. Fokker-Planck equation

It is assumed in the following analysis that the electron distribution is isotropic, in which case the general Fokker-Planck equation takes the form

$$\left(\frac{\partial f}{\partial t}\right)_c = \frac{\Gamma}{v^2} \left[-\frac{\partial}{\partial v} \left(f v^2 \frac{\partial h}{\partial v} + f \frac{\partial g}{\partial v} \right) + \frac{1}{2} \frac{\partial^2}{\partial v^2} \left(f v^2 \frac{\partial^2 g}{\partial v^2} \right) \right], \quad (12)$$

which has been derived by Rosenbluth *et al.*¹⁰ In this equation, f represents the total electron distribution function and v is the electron speed. Hence the electron density n_e is

$$n_e = \int_0^\infty f 4\pi v^2 dv.$$

Also the terms Γ , h , and g are determined by the equations

$$\Gamma = e^4 \ln \Lambda / 4\pi \epsilon_0^2 m_e^2, \\ h(v) = \sum_j \frac{m_e + m_j}{m_j} \left(\frac{4\pi}{v} \int_0^v f_j v'^2 dv' + 4\pi \int_v^\infty f_j v' dv' \right), \quad (13)$$

$$g(v) = \sum_j \frac{4\pi}{3v} \int_0^v f_j v'^2 (3v^2 + v'^2) dv' \\ + \frac{4\pi}{3} \int_v^\infty f_j v' (3v'^2 + v^2) dv'. \quad (14)$$

It is impossible to solve Eq. (12) analytically for a general distribution function, but, if it is assumed that the electron-distribution function is essentially a perturbed Maxwellian (because the containment time is a few times the collision time for electrons), then the equation may be linearized. The effects of the source of electrons created by ionization can be viewed as a perturbation and the total distribution function can be represented by

$$f = \left(\frac{m_e}{2\pi T} \right)^{3/2} n_e \exp\left(-\frac{m_e v^2}{2eT}\right) + f_n,$$

where f_n is the perturbation. The Maxwellian function is a stationary state of the Fokker-Planck equation and hence it makes no contribution to the time derivative on the left-hand side. The perturbation distribution f_n is assumed to be too small to interact with itself via the h and g parameters.

The time-dependent part of the Fokker-Planck equation hence represents the rate of loss of electrons from any element of velocity and real space, which becomes, for electron creation in the ion beam,

$$\left(\frac{\partial f}{\partial t}\right)_c = -S(v) \frac{dN_e}{dt}, \quad (15)$$

where dN_e/dt is the rate of appearance of new electrons per unit volume taking into account their orbitals around the beam axis. The function $S(v)$ represents the velocity distribution of the new electrons at a point in real space arising from their potential energy. It is shown in Appendix B that dN_e/dt depends critically on the initial velocity of creation of the electrons which has been measured experimentally by Rudd and Jorgensen.¹¹ In this instance (see Appendix B)

$$\frac{dN_e}{dt} = nm_b \sigma_i v_b \frac{4r}{\sqrt{\pi} r_0} \frac{e\phi_0}{m_e v_b^2},$$

where ϕ_0 is the potential at r_0 .

The electron velocity distribution, $S(v)$ can be derived from the beam profile and potential distribution. As the main area of interest is near the axis, the Gaussian potential well can be approximated to a parabolic well so that

$$\frac{1}{2} m_e v^2 = e\Delta\phi + \frac{1}{2} m_e w^2 = (e\phi_0/r_0^2)(p^2 - r^2) + \frac{1}{2} m_e w^2,$$

where r is the radius where $S(v)$ is determined and w is the initial electron velocity. The probability of a velocity v depends on the distribution of both w and p as shown in the equation below:

$$S(v) = \frac{\int_0^v f(w)g(p)dw}{4\pi v^2 \int_0^\infty \int_0^v f(w)g(p)dw dv}.$$

It is assumed that $f(w)$ is $2w e^{-w^2/w_0^2}/w_0^2$ where w_0 is the characteristic initial velocity (experimentally $w_0 \approx v_b$) and $g(p)$ is e^{-p^2/r_0^2} , which is derived from the beam profile. As $w_0^2 < 2e\phi_0/m$, integration gives

$$S(v) \approx \frac{1}{2\pi^{3/2}} \left(\frac{m_e}{2e\phi_0}\right)^{1/2} \frac{1}{v^2} \exp\left(-\frac{m_e v^2}{2e\phi_0}\right),$$

which has some similarity to a Maxwellian distribution.

When Eq. (15) is combined with Eq. (12), the Fokker-Planck equation becomes

$$-m_b \sigma v_b \frac{2}{\pi^2} \frac{r}{r_0} \left(\frac{e\phi_0}{m_e v_b^2}\right) \left(\frac{m_e}{2e\phi_0}\right)^{1/2} \frac{\exp(-m_e v^2/2e\phi_0)}{v^2} \\ = \frac{\Gamma}{v^2} \left[-\frac{\partial}{\partial v} \left(f_n v^2 \frac{\partial h}{\partial v} + f_n \frac{\partial g}{\partial v} \right) + \frac{1}{2} \frac{\partial^2}{\partial v^2} \left(f_n v^2 \frac{\partial^2 g}{\partial v^2} \right) \right].$$

It is possible to integrate this equation once by multiplying by $4\pi v^2 dv$ and integrating over the range 0 to v which yields

$$-m_b \sigma v_b \frac{4}{\pi^{1/2}} \frac{e\phi_0 r}{m_e v_b^2 r_0} \operatorname{erf}\left(\frac{m_e v^2}{2e\phi_0}\right)^{1/2} \\ = 4\pi \Gamma \left[-f_n \left(v^2 \frac{\partial h}{\partial v} + \frac{\partial g}{\partial v} \right) + \frac{1}{2} \frac{\partial}{\partial v} \left(f_n v^2 \frac{\partial^2 g}{\partial v^2} \right) \right]. \quad (16)$$

The next integration depends on the functions h and g , which can be derived from Eqs. (13) and (14) and the distribution functions of each species of particle.

1. h function.

There are three species of particles, namely, the main electron distribution, which is Maxwellian, the slow ions, and the beam ions. The distribution functions of the electrons and beam ions are, respectively,

$$f_e = n_e (m_e/2\pi eT)^{3/2} e^{-m_e v^2/2eT}, \quad (17)$$

$$f_b = \delta(v - v_b) \delta(\mu - 1)/4\pi v^2, \quad (18)$$

where δ is the δ function and μ equals $\cos\theta$ in polar coordinates. This anisotropy of the beam must be removed by integration over θ before it can be substituted into Eq. (12), but it is useful to perform this operation after h_b and g_b have been derived in order to improve the accuracy of the expression.

The slow-ion function is more difficult to derive, but it will be shown shortly that the dispersion caused by these particles is unimportant because of the small value of n_i . A simple form for f_i is to assume it to be Maxwellian with a characteristic energy of $e\phi_0$ so that the ion velocity is far smaller than the initial electron velocity. Hence

$$f_i = n_i (m_i/2\pi e\phi_0)^{3/2} e^{-m_i v^2/2e\phi_0}. \quad (19)$$

Substitution of these expressions in Eq. (13) gives

$$h_e = \frac{2n_e}{v} \operatorname{erf}\left(\frac{m_e v^2}{2eT}\right)^{1/2} \\ \approx 2n_e \left\{ \frac{2}{\sqrt{\pi}} \left(\frac{m_e}{2eT}\right)^{1/2} - \frac{2v^2}{3\sqrt{\pi}} \left(\frac{m_e}{2eT}\right)^{3/2} + \dots \right\},$$

$$h_i = m_e n_i / v m_i,$$

as $v \gg (2e\phi_0/m_i)^{1/2}$ and $m_i \gg m_e$, and

$$h_b = \frac{m_e n_b}{2m_b} (v^2 + v_b^2 - 2vv_b\mu)^{-1/2}.$$

This last expression is derived from the expanded version of Eq. (13) given by Rosenbluth *et al.*¹⁰ However, the dependence on μ is inconvenient in the assumed isotropic distribution f_n and maybe eliminated by interaction over all values of μ from 1 to -1 . In this case

$$\bar{h}_b = (m_e n_b / 8m_b v_b v) (|v + v_b| - |v - v_b|).$$

These three expressions for h represent the relative magnitude of the deceleration of the newly created electrons by friction or scattering with the beam ions, slow ions, and the main electron distribution. In view of the mass ratio that enters into this type of effect, it is to be expected that beam ions are virtually ineffective in slowing down the electrons (the beam ions are incapable of producing any deceleration until the electron velocity exceeds that of the beam). In

this case the value of $v^2 \partial h / \partial v$ is

$$v^2 \frac{\partial h}{\partial v} = v^2 \frac{\partial h_e}{\partial v} = \frac{8n_e}{3\pi^{1/2}} v^3 \left(\frac{m_e}{2eT} \right)^{3/2} + \dots \quad (20)$$

2. g function

Using the expressions developed above for f_e , f_i , and f_b , it can be shown with the aid of Eq. (14) that

$$\begin{aligned} g_e &= \frac{n_e}{4v} \left(\frac{2eT}{m_e} \right) \left[\frac{4v}{\pi^{1/2}} \left(\frac{m_e}{2eT} \right)^{1/2} \exp\left(-\frac{m_e v^2}{2eT}\right) \right. \\ &\quad \left. + 2 \left(1 + \frac{m_e v^2}{eT} \right) \operatorname{erf}\left(\frac{m_e v^2}{2eT}\right)^{1/2} \right] \\ &\approx \frac{n_e}{4} \left(\frac{2eT}{m_e} \right)^{1/2} \left[\frac{8}{\pi^{1/2}} + \frac{8}{3\pi^{1/2}} \frac{m_e v^2}{2eT} \right. \\ &\quad \left. + \frac{1.47}{\pi^{1/2}} \left(\frac{m_e v^2}{2eT} \right)^2 + \dots \right], \end{aligned}$$

$$g_i \approx n_i v \text{ if } v \gg (2e\phi_0/m_i)^{1/2},$$

$$g_b = \frac{1}{2} n_b (v^2 + v_b^2 - 2vv_b\mu)^{1/2}.$$

Hence by averaging over all values of μ , we have

$$\bar{g}_b = \frac{n_b}{12vv_b} (|v+v_b|^3 - |v-v_b|^3).$$

Again the scattering effects of the slow ions may be neglected but the scattering caused by the electron distribution and the beam ions are comparable and both must be included. The scattering represented by the g expression will cause the average energy of the newly created electrons to rise. In first order the derivative of g with velocity is

$$\frac{\partial g}{\partial v} = \frac{\partial g_e}{\partial v} + \frac{\partial g_b}{\partial v} = \frac{4n_e}{3\pi^{1/2}} \left(\frac{m_e v}{2eT} \right) \left(\frac{2eT}{m_e} \right)^{1/2} + \frac{n_b v}{3v_b}. \quad (21)$$

B. Perturbed distribution function

With the values of g and h in Eqs. (20) and (21), it is possible to solve Eq. (16), which gives on integration

$$\begin{aligned} f_n v^2 \frac{\partial^2 g}{\partial v^2} \exp\left(-2 \int_v \frac{v'^2 \partial h / \partial v' + \partial g / \partial v' dv'}{v'^2 \partial^2 g / \partial v'^2}\right) \\ + \frac{2nm_b\sigma v_b r}{4\pi\Gamma r_0} \frac{4}{\pi^{1/2}} \frac{e\phi_0}{m_e v_b^2} \int_v \operatorname{erf}\left(\frac{m_e u^2}{2e\phi_0}\right)^{1/2} \exp\left(-2 \int_u \frac{v'^2 \partial h / \partial v' + \partial g / \partial v'}{v'^2 \partial^2 g / \partial v'^2} dv'\right) du = \text{const.} \end{aligned}$$

Substitution of Eqs. (20) and (21) shows that $v^2 \partial h / \partial v$ is unimportant compared with $\partial g / \partial v$, which suggests that the deceleration of the newly created electrons is unimportant compared with the scattering collisions. In this case the above equation may be simplified to

$$\begin{aligned} f_n \frac{\partial^2 g}{\partial v^2} + \frac{2nm_b\sigma v_b r}{4\pi\Gamma r_0} \frac{4}{\sqrt{\pi}} \frac{e\phi_0}{m_e v_b^2} \\ \times \int_v \operatorname{erf}\left(\frac{m_e u^2}{2e\phi_0}\right)^{1/2} \frac{du}{u^2} = \text{const.} \end{aligned}$$

If u is small, then

$$\begin{aligned} f_n = C - \frac{nm_b\sigma v_b r}{4\pi\Gamma r_0} \frac{8}{\pi} \left(\frac{2e\phi_0}{m_e} \right)^{1/2} \\ \times \frac{\ln v}{v_b^2} \left[\frac{4n_e}{3\pi^{1/2}} \left(\frac{m_e}{2eT} \right)^{1/2} + \frac{n_b}{3v_b} \right]^{-1}. \end{aligned}$$

The constant C is of some importance as no sink of electrons has been postulated. A natural sink exists when v is of the order of the thermal velocity of the electrons as then the two distributions cannot be distinguished. If f_n is zero when v equals v_s , then

$$f_n = A \ln(v_s/v),$$

where

$$A = \frac{nm_b\sigma v_b r}{4\pi\Gamma r_0} \frac{8}{\pi} \left(\frac{2e\phi_0}{m_e v_b^2} \right)^{1/2} \left[\frac{4n_e}{3\pi^{1/2}} \left(\frac{m_e}{2eT} \right)^{1/2} + \frac{n_b}{3v_b} \right]^{-1}. \quad (22)$$

The total number density of these electrons can be found by integration over velocity space, which gives

$$n_n = \int_0^{v_s} f_n 4\pi v^2 dv = \frac{4}{3} \pi A v_s^3.$$

When v_s is less than $(2eT/m_e)^{1/2}$ this density is considerably smaller than n_e . It is difficult to determine the value of v_s precisely, but if v equals v_s when the scattering time for these new electrons with themselves is equal to the scattering time for collisions between new electrons and the main distribution, then v_s is approximately $\frac{1}{2}(2eT/m_e)^{1/2}$ although this velocity depends on the gas and beam densities. An illustration of the distribution function is shown in Fig. 3 where the perturbation appears as a spike on the Maxwellian distribution function at $v=0$. The effect of the uncertainty in the value of v_s does not influence the energy transfer, however, as will be seen in Sec. IV C.

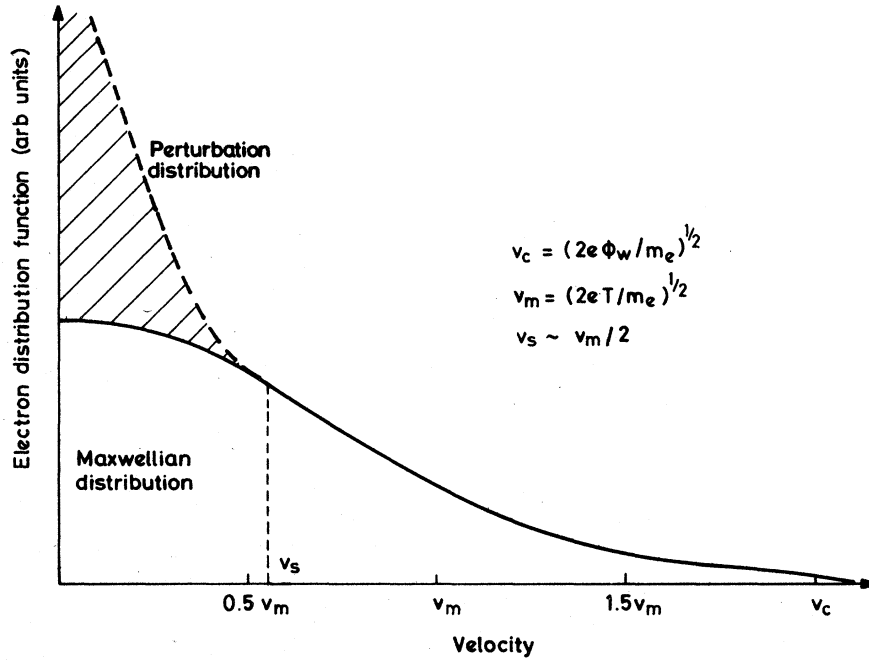


FIG. 3. Detailed shape of the electron distribution including the effects of newly created electrons.

C. Beam energy balance

The deceleration of the beam is governed by an equation of the type

$$\frac{\partial v_b}{\partial t} = \Gamma_b \frac{\partial H}{\partial v_b},$$

where

$$\Gamma_b = e^4 \ln \Lambda / 4\pi \epsilon_0^2 m_b^2$$

and

$$H(v_b) = \sum_j \frac{m_b + m_j}{m_b} \left(\frac{4\pi}{v_b} \int_0^{v_b} v'^2 f_j dv' + 4\pi \int_{v_b}^{\infty} v' f_j dv' \right).$$

The slow ions are ineffective in regarding the beam ions because of their high mass, but both electron distributions can cause deceleration. Substitution of f_m and f_n in the above equation yields

$$H = \frac{m_b}{m_e} \left[\frac{n_e}{v_b} \operatorname{erf} \left(\frac{m_e v_b^2}{2eT} \right)^{1/2} + 4\pi A \left(-\frac{5v_b^2}{36} - \frac{v_b^2}{6} \ln \left(\frac{v_s}{v_b} \right) + \frac{v_s^2}{4} \right) \right].$$

If the electron temperature is high, then the contribution from the main distribution is small (because $w > v_b$) and hence can be neglected. Substitution of experimental values shows that only 10% of the total energy input to the electrons comes from this channel. Hence, in this case, the rate of change of beam energy is

$$\frac{dU_b}{dt} = 2m_b v_b \frac{dv_b}{dt} = -4\pi A m_b \frac{v_b^2}{3} \frac{m_b \Gamma_b}{m_e} \left(2 \ln \frac{v_s}{v_b} + \frac{4}{3} \right)$$

and

$$\frac{dW_e}{dt} = -n_b \frac{dU_b}{dt} = \frac{4\pi}{3} A n_b \frac{m_b^2 v_b^2}{m_e} \Gamma_b \left(2 \ln \frac{v_s}{v_b} + \frac{4}{3} \right). \quad (23)$$

The value of v_s has little effect on the energy transfer.

The last stage involves the integration of the energy absorbed in a unit volume at r , represented by dW_e/dt , over all radii, which is equal to the total energy removed by the flux of escaping ions. This balance may be represented by the expression

$$\int_0^{\infty} m_b \sigma_i v_b e \phi_w \exp \left(-\frac{\beta^2 r^2}{r_0^2} \right) 2\pi r dr = \int_0^{\infty} \frac{dW_e}{dt} 2\pi r dr.$$

This integration is necessary because the electron-electron energy transfer time is considerably shorter than the containment time. It is not possible to solve exactly the right-hand side of the above equation, but the term A can be expanded as a series function of the ratio n_b/n_e . Hence after simplification, we have

$$\frac{\phi_w}{1 + \beta^2} = \frac{2\phi_0^{1/2} T^{1/2} n_{b0}}{[2 - \frac{1}{2}(1 + \beta^2)] n_{e0}} \left[2 \ln \left(\frac{v_s}{v_b} \right) + \frac{2}{3} \right] \times \left[1 - \frac{(\frac{3}{2} - \frac{1}{2}\beta^2)}{(2 - \beta^2)} \frac{\pi^2 n_{b0}}{4 n_{e0}} \left(\frac{2eT}{m_e v_b^2} \right) + \dots \right].$$

The higher-order terms in n_{b0}/n_{e0} may be collected

to give

$$\frac{\phi_w}{1+\beta^2} \approx \frac{2\phi_0^{1/2} T^{1/2}}{2-\frac{1}{2}(1+\beta^2)} \frac{n_{b0}}{n_{e0}} \left[2 \ln \left(\frac{v_s}{v_b} \right) + \frac{2}{3} \right] \\ \times \left(1 - \frac{\pi^{1/2}}{10} \frac{n_{b0}}{n_{e0}} \frac{2eT}{m_e v_b^2} \right),$$

if $\beta \approx 0.33$ (see Sec. IV D). The small value of n_b/n_e at large values of r attenuates the second term considerably and at high pressures (greater than 10^{-4} Torr), it can be neglected completely.

D. β parameter

β^2 has been a free parameter in the model, although an exact theory could determine β^2 via a numerical solution of an integrodifferential equation based on velocity space diffusion and energy balance. The approach adopted here is considerably simpler and offers a greater insight into the meaning of the β parameter.

In Sec. III B, β^2 was to be determined by the equality between the radial dependence of n_e in Eqs. (10) and (11). This demands that

$$\exp[-(1+\beta^2)r^2/2r_0^2] = [(\phi + \phi_w)/\phi_w] e^{\phi/T},$$

where ϕ is the potential relative to the center of the beam. Hence, near the axis where ϕ is small

$$-\frac{(1+\beta^2)r^2}{2r_0^2} = \frac{\phi}{T} \approx -\frac{\phi_w}{T} (1 - e^{-(\beta r/r_0)^2}). \quad (24)$$

If n_{e0} is approximately equal to n_{b0} and only the first term of the series expansion of the exponential in Eq. (24) is considered then the above equality becomes:

$$\frac{1+\beta^2}{2} = \left(\frac{2\beta(1+\beta^2)(1 - e^{-\beta^2})^{1/2}}{\frac{1}{2}(3-\beta^2)} \right) \left[2 \ln \left(\frac{v_s}{v_b} \right) + \frac{2}{3} \right]^2.$$

The solution to this is $\beta^2 = 0.33$ when v_s/v_b equals 1.4 although β is relatively invariant to the value of v_s/v_b .

With this calculated value of β^2 , it is possible to write

$$\phi_w = 2.02 \left(\frac{n_{b0}}{n_{e0}} \right)^2 T \left(1 - 0.4 \frac{n_{b0}}{n_{e0}} \frac{w}{v_b} \right)^2. \quad (25)$$

If this equation is combined with Eq. (11), it is possible to eliminate T giving

$$n_{e0} = 0.33 \pi \epsilon_0^2 (em_e)^{1/2} n_{e0} v_b \phi_w^{3/2} / e^3 \ln(\Lambda). \quad (26)$$

E. Radial and axial energy transfer

It has been assumed, hitherto, that the beam is perfectly collimated and the electron temperature is uniform everywhere. It will be shown here that a Gaussian beam profile allows the expressions developed for perfectly collimated beams to be extended to divergent beams. In addition the value of β^2 derived in Sec. IV D allows the local rate of energy absorption dW_e/dt to have

exactly the same radial scaling as the energy loss caused by the outward drift of the electrons.

1. Axial energy transfer

The effects of beam divergence cause an axial variation of ϕ_w , producing a broad shallow well where the beam is wide which is transformed into a deep narrow well near the beam extraction region. The electrons can move axially along the well oscillating between contours of constant potential. The electron production rate Q_e , in a zone $d\phi$ at potential ϕ for a local beam density n_b , is

$$Q_e = n m_b \sigma v_b 2\pi r \frac{dr}{d\phi} d\phi.$$

For a beam and potential well which are both Gaussian

$$\phi = \phi_w e^{-(\beta r/r_0)^2},$$

$$n_b = n_{b0} e^{-r^2/r_0^2} = n_{b0} (\phi/\phi_w)^{1/\beta^2},$$

and

$$dr/d\phi = r_0^2/2r\beta^2\phi,$$

where ϕ is in this case the binding potential of the electrons and is measured from the remote walls which are at constant potential. Hence

$$Q_e = n \sigma_i n_{b0} v_b \frac{\pi r_0^2}{\beta^2 \phi} \left(\frac{\phi}{\phi_w} \right)^{1/\beta^2} d\phi.$$

However, the beam current remains constant along the beam axis so that

$$I_b = \pi n_{b0} v_b e r_0^2$$

and

$$Q_e = \frac{n \sigma I_b}{\beta^2 e \phi} \left(\frac{\phi}{\phi_w} \right)^{1/\beta^2} d\phi.$$

Hence if the beam current and gas density are constant along the beam axis then the production rate of electrons along a contour of constant potential is the same irrespective of beam size. Hence there is no axial flow of electrons and the energy balance of an axial segment of the beam can be considered as if it were infinitely long and of the same radius. This arises from the Gaussian profile of the beam which in turn generates a similar potential distribution. In this state the flow of particles (and hence energy) along the axis is zero.

2. Radial transfer

The energy absorbed per unit volume by the electron distribution is determined by the function dW_e/dt . This energy is absorbed by the local electrons and enables them to drift outwards against the electric field. If the radial dependence of dW_e/dt and the energy required to main-

tain this drift are the same, then this implies that there is no temperature gradient because the local energy absorption and loss are the same everywhere. From Eq. (23) the radial scaling of dW_e/dt is

$$\frac{dW_e}{dt} = C' \frac{r}{r_0} \exp\left(-\frac{2r^2}{r_0^2}\right) \exp\left(\frac{(1+\beta^2)}{2} \frac{r^2}{r_0^2}\right),$$

where C' contains all terms that are not functions of r . The energy required for drift against the field is $n_e E(dr/dt)_d$, where E is the local electric field and $(dr/dt)_d$ is the drift velocity. An approximate expression for this velocity is

$$\left(\frac{dr}{dt}\right)_d \simeq n_b n \sigma_i v_b r_0 / n_e.$$

Hence the radial dependence of this energy loss is

$$\text{loss rate} = m_{b0} \sigma_i v_b r_0 \frac{2\phi_w r}{r_0^2} \exp\left(-\frac{\beta^2 r^2}{r_0^2}\right) \exp\left(-\frac{r^2}{r_0^2}\right).$$

These two radial expressions are exactly the same provided

$$1.5 - \frac{1}{2}\beta^2 = 1 + \beta^2$$

or

$$\beta^2 = 0.33.$$

This value of β^2 is in exact agreement with the value derived in Sec. IV D from a completely different concept.

Hence it can be seen that there will be a strong tendency for a beam of any arbitrary profile to relax into a Gaussian shape where β^2 is 0.33. This profile eliminates any need for axial or radial energy transport and hence is an equilibrium state for the beam plasma.

V. POISSON'S EQUATION

The electrostatic potential can be derived from the charge densities and electron temperature by two methods. The exact method is to solve the full Poisson equation in cylindrical geometry, which will be done in a following section. A less accurate technique involves the assumption of plasma neutrality so that $d^2\phi/dr^2$ and $d\phi/dr$ are neglected and Poisson's equation reduces to

$$n_b + n_i = n_e,$$

which is the plasma equation. Harrison and Thompson¹² have solved the plasma equation when n_b is zero and Green⁷ has produced solutions where n_b is finite and uniform. This equation will give a detailed spatial solution when the Boltzmann distribution for electrons is assumed (i.e., $n_e = n_{e0} e^{+\phi/T}$). The validity of the plasma equation is doubtful, however, at low pressure because of the dominant effects of the beam ions and the high potential gradients in the plasma.

A much simpler solution of the plasma equation is described by Gabovich *et al.*, where only axial plasma neutrality is assumed and all radial variation in density is neglected. This determines the magnitude of the potential well but not its shape. A similar technique will be used in Sec. V A to obtain an approximate estimate for the scaling of ϕ_w .

A. Neutral plasma solution

The basic expression equates n_{e0} to $n_{i0} + n_{b0}$, hence from Eqs. (3) and (26) one obtains

$$0.33 \frac{\phi_w^{3/2} \pi \epsilon_0^2 (em_e)^{1/2} n \sigma_i v_b}{e^3 \ln \Lambda} = \left(\frac{m_i}{2e\phi_w}\right)^{1/2} \frac{n_{b0} n v_b \sigma r_0}{1 - \exp(-\beta^2)} + n_{b0}. \quad (27)$$

The above equation relates the potential to the gas density and beam density and indicates that, at low pressures,

$$\phi_w = \left(\frac{n_{b0}}{n}\right)^{2/3} \left(0.33 \pi \sigma_i v_b \epsilon_0^2 \frac{(m_e e)^{1/2}}{e^3 \ln \Lambda}\right)^{-2/3}, \quad (28a)$$

and at high pressures,

$$\phi_w^2 = n_{b0} r_0 \frac{\sigma}{\sigma_i} \left(\frac{m_i}{m_e}\right)^{1/2} \frac{e^2 \ln \Lambda}{0.33 \pi \epsilon_0^2} \frac{1}{1 - \exp(-\beta^2)}. \quad (28b)$$

These two equations show that ϕ_w decreases with increasing pressure until a lower limit is reached, which is determined by the production rate of the slow ions. Furthermore at low pressures, the beam potential depends solely on the beam density and is independent of the beam radius. This scaling differs completely from the scaling of the potential of a vacuum beam, where

$$\phi_{wv} \propto n_b r_0^2.$$

This effect may be exploited to produce an extremely collimated beam whose divergence is only limited by its finite emittance. These results are mentioned in Sec. VI C and are discussed in greater detail elsewhere (Holmes and Thompson¹³).

At high gas target thicknesses, a large fraction of the ion beam (dependent on the beam energy) will be converted into neutral atoms and this neutral atom beam cannot create a potential well. This fast neutral beam is a source of plasma and therefore a sheath appears at the plasma boundary (i.e., the walls). Dunn and Self⁶ have discussed this problem in detail for finite temperature electrons in electron beams. This treatment has been extended by Green⁷ to intense ion beams. Hence by a simple modification of the model to incorporate the relative magnitudes of n_{b0} to n_{n0} the fast neutral density, it can be shown that at low pressure

$$\phi_{wi} = \phi_w [(n_{n0} + n_{b0})/n_{b0}]^{2/3},$$

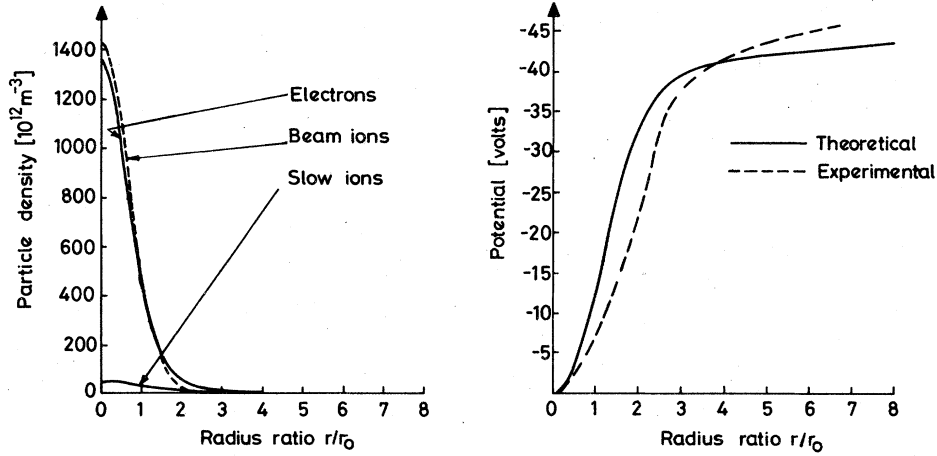


FIG. 4. Shape of the potential well and particle profiles at low pressure; beam energy 20-keV He⁺, pressure 1.25×10^{-4} Torr, current 17.6 mA, radius 5 mm.

and at high pressure

$$\phi_{wi} = \phi_w [(n_{n0} + n_{b0}) / n_{b0}],$$

where ϕ_{wi} is the potential generated by a pure ion beam of density $n_{b0} + n_{n0}$.

B. Numerical solution

Poisson's equation in cylindrical geometry is of the form

$$\frac{d^2 \phi}{dr^2} + \frac{1}{r} \frac{d\phi}{dr} = -\frac{e}{\epsilon_0} (n_i + n_b - n_e), \quad (29)$$

where there is azimuthal and axial uniformity in potential. Each charge species has a different spatial distribution that is described by Eqs. (2), (7), and (11), and these can be introduced into Eq. (29). This discussion is limited to a Gaussian beam profile which is the steady state solution following the arguments advanced in Secs.

IV D and IV E. However, it is easy to apply this technique (assuming that the other particle profiles are independent) to other primary beam profiles. For a Gaussian beam, however, Eq. (29) becomes

$$\frac{\epsilon_0}{e} \left(\frac{d^2 \phi}{dr^2} + \frac{1}{r} \frac{d\phi}{dr} \right) = - \left[\frac{n\sigma v_b (m_i)^{1/2}}{r} \int_0^r \frac{n_{b0} e^{-a^2/r_0^2} a da}{[\phi(a) - \phi(r)]^{1/2}} + n_{b0} e^{-r^2/r_0^2} - n_{e0} (\phi_w + \phi) e^{(\phi/T)} / \phi_w \right].$$

This equation may be simplified slightly by the introduction of the variables $x = r/r_0$ and $y = \phi/\phi_0$. Hence

$$-\frac{\epsilon_0 \phi_0}{er_0^2} \left(\frac{d^2 y}{dx^2} + \frac{1}{x} \frac{dy}{dx} \right) = \frac{n_{i0}}{x} \int_0^x \frac{e^{-x'^2} x' dx'}{(y' - y)^{1/2}} - n_{e0} e^{\phi_0 y/T} \left(\frac{\phi_w + y\phi_0}{\phi_w} \right) + n_{b0} e^{-x^2}. \quad (30)$$

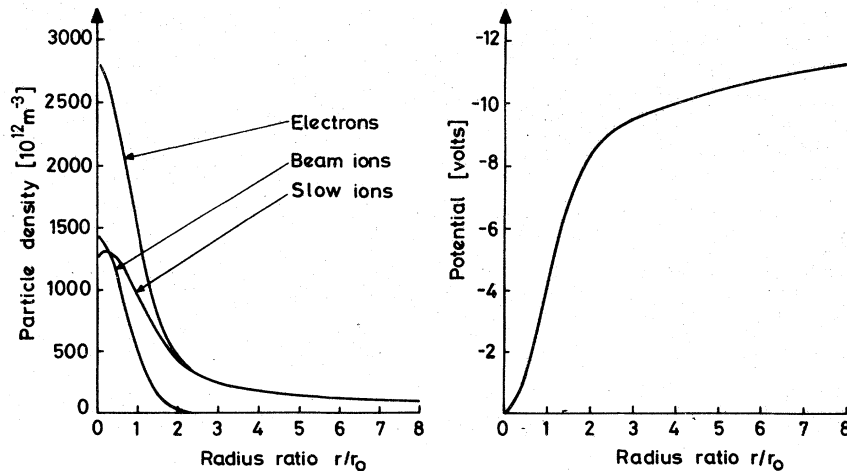


FIG. 5. Shape of the potential well and particle profiles at high pressure; beam energy 20-keV He⁺, pressure 2×10^{-3} Torr, current 17.6 mA, radius 5 mm.

It is possible to solve this integrodifferential equation using a finite-step technique to approximate the differentials. However, a single solution to Poisson's equation is insufficient to determine the well potential because n_{e0} , T , and n_{i0} are all functions of ϕ_w . Hence a relaxation routine must also be included in the numerical solution so that the value of ϕ_w derived from Poisson's equation is used to modify the initial estimates for n_{e0} , T , and n_{i0} . The final numerical solution is shown in Figs. 4 and 5 where particle and potentials distributions in both pressure regimes are shown.

It can be seen that the three charged-particle distributions and the potential well are all of Gaussian form, although with different radii. The shape of the numerical potential well supports the arguments advanced in Sec. III B.

VI. EXPERIMENTAL RESULTS

A series of experiments has been performed on a helium beam moving at constant energy through a helium gas cell. An illustration of the apparatus is shown in Fig. 6. The beam is produced by a four electrode extraction system which has been described by Thompson¹⁴ and the current density and divergence angle of the beam may be controlled by varying the plasma density in the source. No magnetic focussing of the beam is used. The beam plasma is isolated from the extraction electrodes by the last electrode gap, which creates a potential to reflect the electrons back into the plasma. Thus the beam plasma is surrounded by surfaces at a uniform potential (in this case these surfaces are earthed) and electrons can only escape by velocity space diffusion.

Two techniques are used to examine the space-charge potential. First, the plasma potential may be measured using a "hot" Langmuir probe, described by Gabovich.⁴ The bias voltage rela-

tive to the earthed wall required to give zero wall current from the probe is equal to the local plasma potential. Second, a shielded probe with a grid may be used to make an energy analysis of the particles which are expelled radially from the beam. This probe does not give a spatial resolution of the potential well and can only determine the electron temperature and maximum well potential from the energy distribution of the slow ion current. It has the advantage that it does not enter the beam and hence can work at high beam energies.

A. Potential well

The plasma potential at a point in the beam is defined as the voltage between the measurement point and the beam axis and is equal to the difference between the floating potential of the probe at the two points if the electron temperature is constant. Any thermionic emission from the probe caused by beam heating is limited by the beam plasma density and hence the alteration in floating potential is independent of position. However, the plasma potential must be corrected for the effects of charge exchange neutralization.

The Langmuir probes shown in Fig. 6 have been constructed of tantalum and alumina to withstand the beam heating up to beam energies of the order of 25 keV. They have been used to measure the dependence of the potential on the main beam parameters, in particular the gas density, beam radius and beam energy.

In Figs. 7 and 8, the well potential is shown as a function of gas density for helium beams in helium, hydrogen, and argon. These curves show that the potential decreases with increasing gas pressure and then remains constant at high pressures. The experimental data and theory agree well over the entire pressure range for each gas.

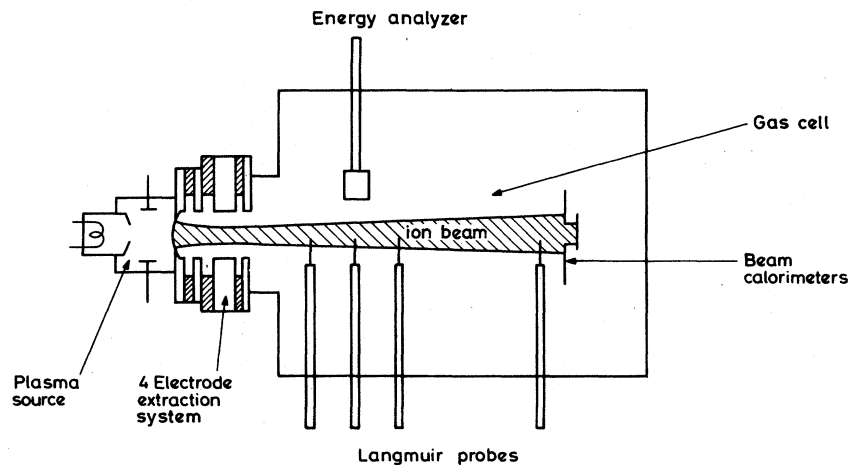


FIG. 6. Beam line.

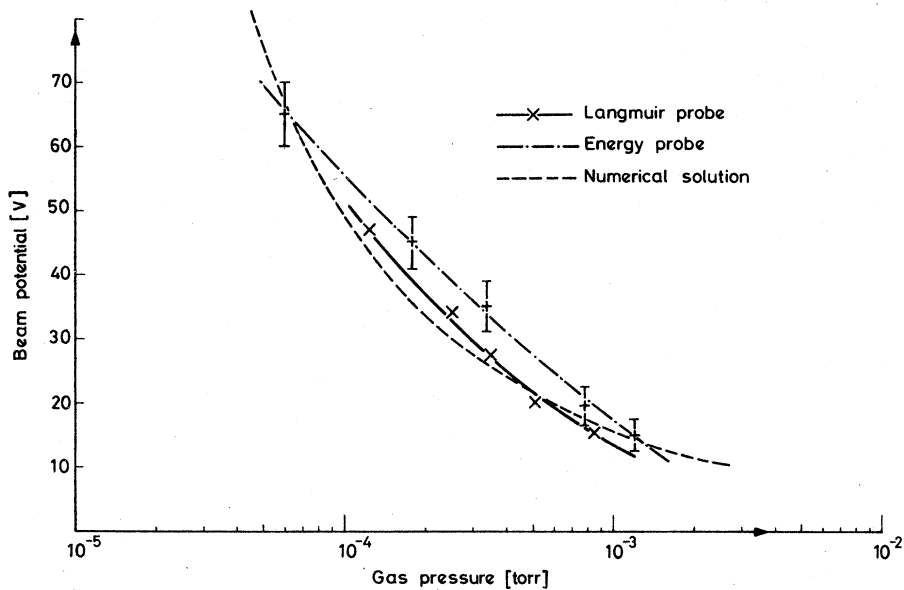


FIG. 7. Beam potential ϕ_w as a function of gas pressure; beam energy 20-keV He^+ , beam radius 5 mm, current 17.6 mA.

The change in the scaling of the potential with pressure occurs when the slow ion density exceeds the beam ion density so that the electron density has to neutralize the space charge of the slow ions instead of the beam. In Fig. 9, the theoretical peak slow ion and electron densities are plotted as a function of pressure for the experimental beam used to obtain the data shown in Fig. 7. It can be seen that n_{i0} increases al-

most linearly with pressure whereas n_{e0} only rises slowly at low pressure and then more rapidly as n_{i0} becomes greater than n_{b0} .

The limiting value of ϕ_w at high pressures scales $(\sigma m_i^{1/2} / \sigma_i)^{1/2}$, which depends strongly on the atomic species of the neutralizing gas. This scaling can be used as an indirect test of the validity of the model by comparing the values obtained from the well potential with published data

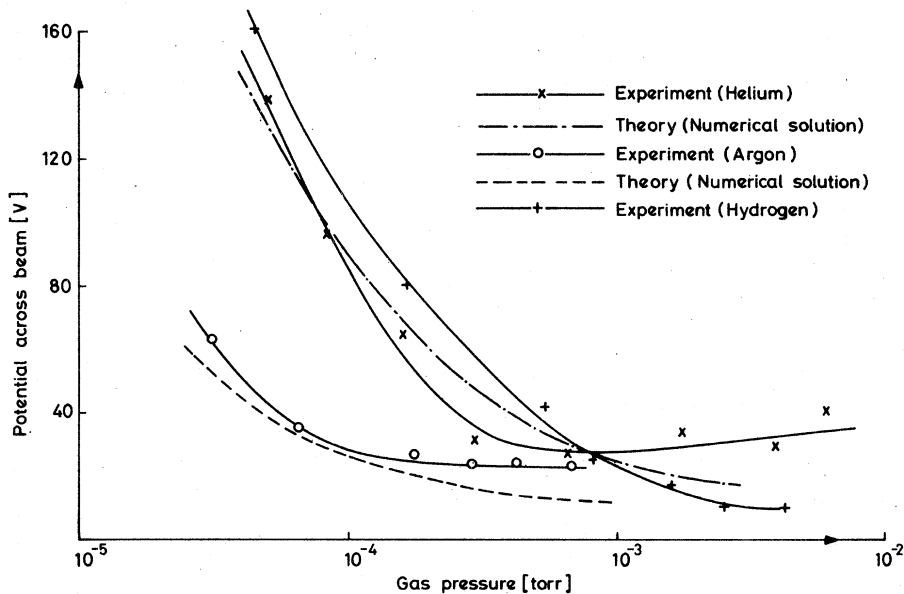


FIG. 8. Beam potential ϕ_w as a function of gas pressure; beam energy 20-keV He^+ , beam radius 1.4 mm, current 10 mA.

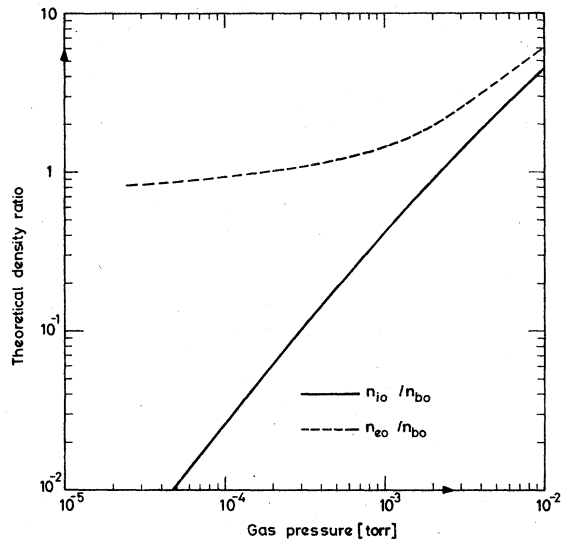


FIG. 9. Ratio of electron or ion density as a function of pressure; beam energy 20-keV He⁺, current 17.6 mA.

on the cross sections. Using the data from Fig. 7, the low limit for ϕ_w yields the following cross-section ratios, $\sigma_1\sigma_{i2}/\sigma_2\sigma_{i1}$, which are in fair agreement with published data, from Refs. 15 and 16 where σ_1 and σ_2 are the sum of σ_i and σ_{i0} for the two gases used to derive the ratio:

	Experimental data	Published data
He/Ar	5.2	5.1
He/H ₂	6.9	7.9
H ₂ /Ar	0.76	0.64

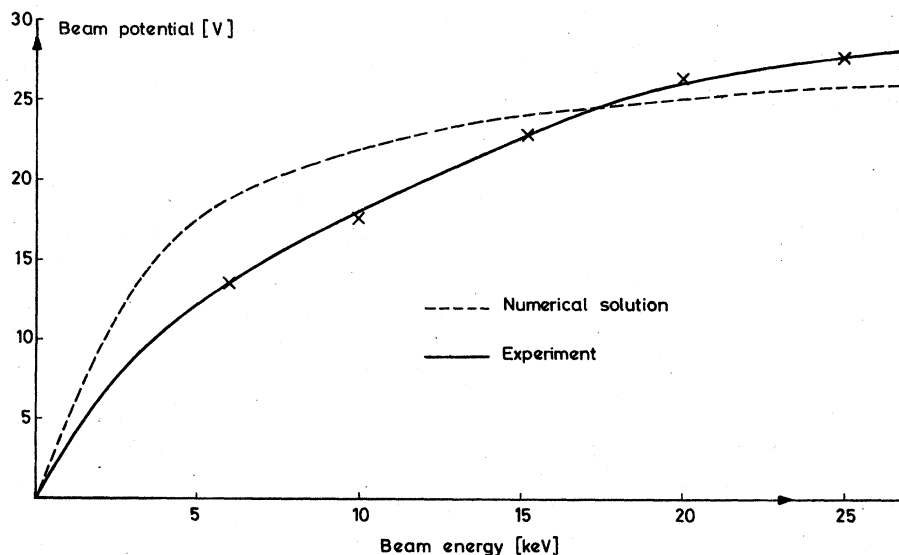


FIG. 10. Beam potential ϕ_w as a function of beam energy; current 17.6 mA, beam radius 5 mm, pressure 7×10^{-5} Torr.

The variation of the well potential with beam energy is shown in Fig. 10. The theoretical curve includes the effects of the variation of the cross sections with beam energy and agrees fairly closely with experiment.

The dependence of the potential well on beam current and beam radius is difficult to analyze experimentally because the beam divergence is a function of the beam current for a given extraction system at constant beam energy and pressure. However, if the beam potential is measured at various points along the axis of a diverging beam it is possible to derive the potential at several different radii and this is shown in Fig. 11. The beam radius is found from the beam divergence, measured using a set of calorimeters. The experimental dependence of the beam potential is virtually $r^{-1.6}$ and agrees well with theory.

B. Energy analysis

The main method of operation of this probe is to use the grid as a filter so that only ions or electrons are allowed to reach the collector. The energy of these particles that pass through the grid can then be analyzed by biasing the collector and measuring the collected current.

The electron temperature T may be easily found with this probe by plotting current-voltage characteristic on log-linear axes and measuring the slope. In Fig. 12 the dependence of T on gas density is shown which has a pronounced minimum at around pressures of 10^{-3} Torr and agrees well with theory. It can be seen in Fig. 9 that the minimum value of T coincides with the pressure where n_{i0} equals n_{b0} .

The ion current-voltage characteristic can be

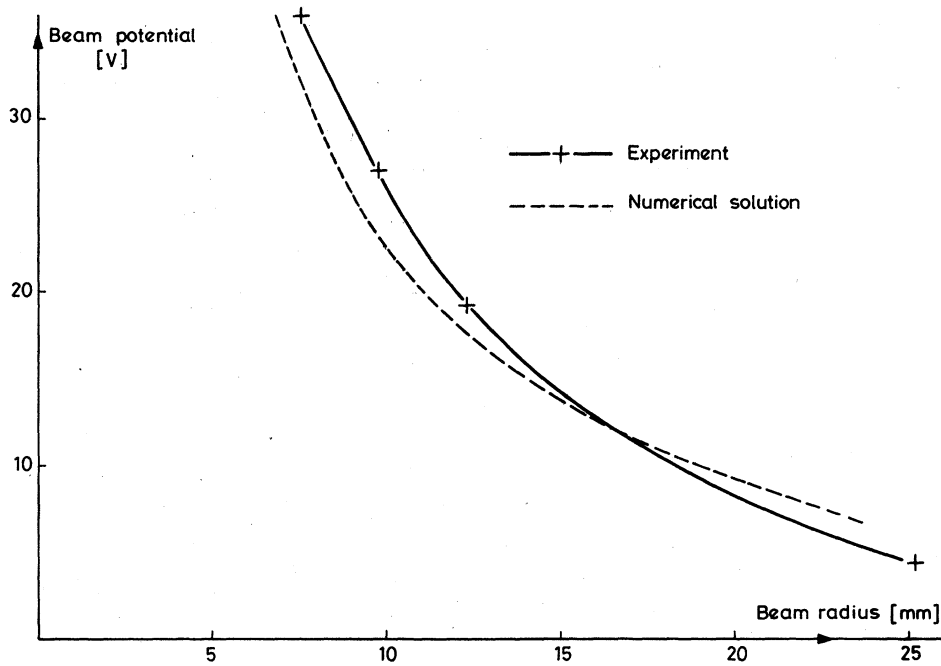


FIG. 11. Beam potential ϕ_w as a function of beam radius; current 17.6 mA, beam energy 20 keV He⁺, pressure 7×10^{-5} Torr.

used to obtain an estimate for ϕ_w and β^2 . However, repulsion of the electrons from the grid creates a space-charge potential that causes an offset between the collector potential and the ion energy. The shape of the characteristic and noting the potential at which the current saturates,

enables an approximate value for ϕ_w and β^2 to be derived.

The dependence of ϕ_w with gas pressure is shown in Fig. 7 where it agrees closely with the Langmuir-probe data. In Fig. 13 the dependence of β on gas density is shown. The value of β de-

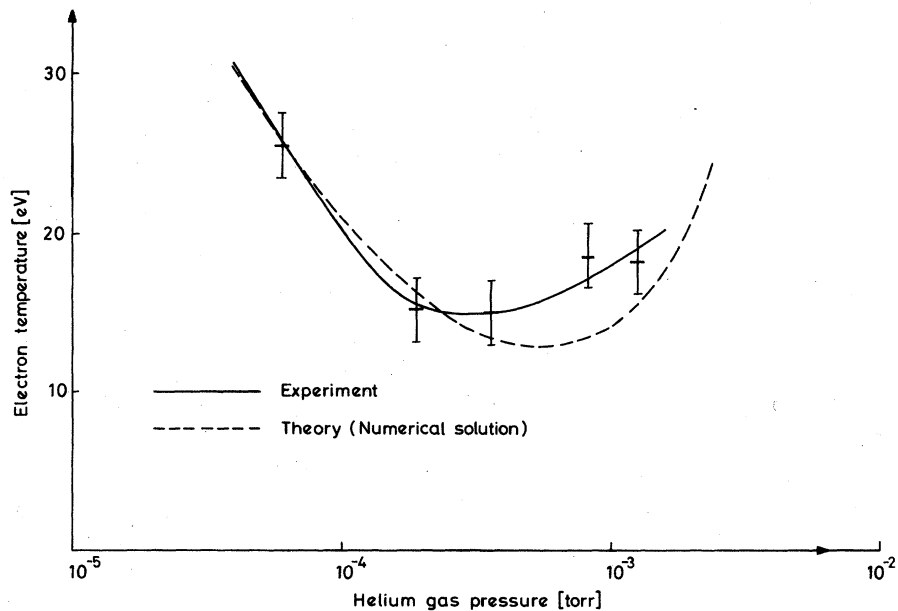


FIG. 12. Electron temperature as a function of pressure; beam energy 20-keV He⁺, beam radius 5 mm, current 17.6 mA.

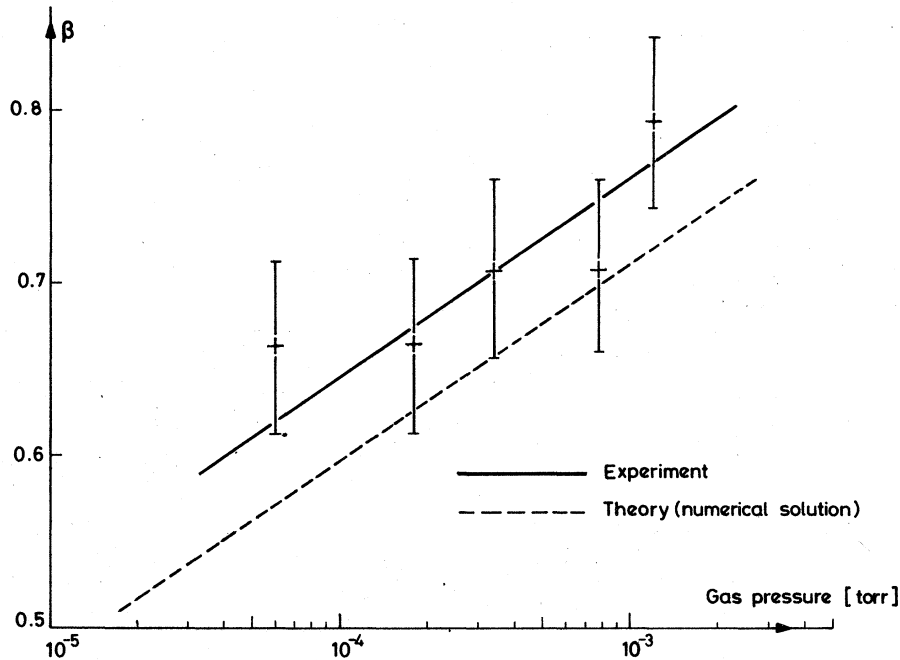


FIG. 13. Radius ratio β as a function of pressure; beam energy 20-keV He⁺, current 17.6 mA, radius 5 mm.

derived from the numerical solution of Poisson's equation is also shown on the same graph and fairly good agreement is obtained. The very slow change of β with gas density is caused by change in the value of n_{e0}/n_{p0} from unity which can be seen in Fig. 9. This would affect the value of β^2 derived in Eq. (24).

C. Beam divergence

Only a very limited description of the beam envelope is presented here and a more detailed discussion of the effects of space charge neutralization on the beam envelope will be published later. The radial electric field derived in Sec. IV can be combined with the beam envelope equation developed by Kapchinskij and Vladimirskij¹⁷ to provide a complete description of the beam envelope and beam divergence. The form of the equation shows that the divergence angle is approximately proportional to the radial electric field. Hence it is possible to compare the relative divergences of a vacuum (or unneutralized) beam and a neutralized beam by comparing the scalings of the electric field. These are, respectively, for the vacuum beam

$$E \propto n_{p0} r_0,$$

and for the neutralized beam

$$E \propto (n_{p0}/n)^{2/3} (1/r_0),$$

which shows that the field of the neutralized beam

decreases with increasing beam envelope radius unlike the vacuum beam. Hence it is expected that the divergence will decrease with increasing beam radius at constant beam density. This leads to the surprising conclusion that large-diameter high-current ion beams have lower divergences than small-diameter low-current beams.

This conclusion has been tested experimentally using the apparatus described in Sec. VI. The plasma source was a reflex arc source operated in low magnetic field to produce a quiescent plasma. The divergence was measured using a set of calorimeters which eliminates any uncertainties caused by electron collection or emission when electrical measurements of divergence are made. The results are shown in Fig. 14 and it can be seen that the divergence of a helium beam decreases with increasing extraction aperture radius. The perveance density (electron perveance) and gas density were approximately constant over the entire series of measurements being, respectively, $5.3 \times 10^{-7} \text{ A V}^{-3/2} \text{ cm}^{-2}$ and $6 \times 10^{-4} \text{ Torr}$.

The scaling of the lowest curve with beam energy suggests that the 6-mm-radius beam has attained the fundamental emittance limit so that the space-charge forces are less powerful than the finite ion temperature T_{ib} , which causes a divergence of $(T_{ib}/V_b)^{1/2}$ radians and results in an intense ion beam with a normalized brightness of $3 \cdot 10^{12} \text{ mA cm}^{-2} \text{ sr}^{-1}$.

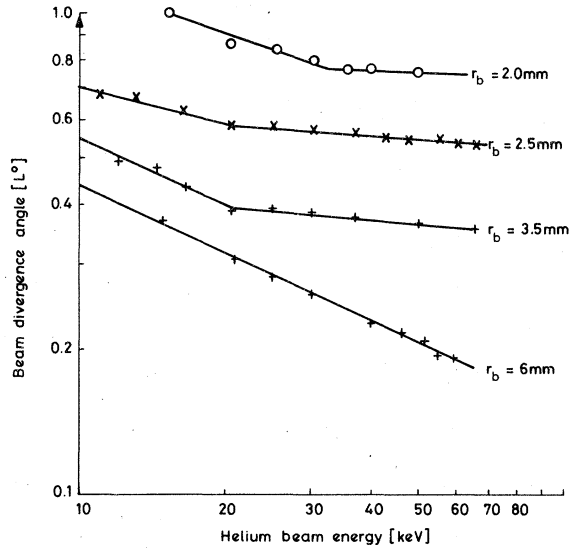


FIG. 14. Beam divergence as a function of beam energy and beam radius for a He⁺ beam.

VII. CONCLUSIONS

A theoretical model for the behavior of the beam plasma in intense ion beams including both the particle and energy balance has been developed, the results of which are in good agreement with experiment. The behavior of the beam plasma has suggested methods by which the plasma potential can be reduced, either by increasing the gas density or by increasing the beam diameter.

This last method is extremely useful since the residual divergence of the ion beam can be reduced by increasing the perveance. The large 6-mm-radius beam is virtually space charge free and of very high brightness. It can be easily utilized in controlled thermonuclear-fusion research work for diagnostics or neutral injection.

ACKNOWLEDGMENTS

The author would like to thank Dr. E. Thompson, Dr. T. S. Green, and Dr. J. G. Cordey for many useful discussions and also G. L. Verra for his aid on the numerical solution to the problem.

APPENDIX A

In Sec. III A it was assumed that the potential could be represented by a series of the form

$$-\phi(r) = \phi_0 \frac{r^m}{r_0^m} + \phi_1 \frac{r^{m+1}}{r_0^{m+1}} + \phi_2 \frac{r^{m+2}}{r_0^{m+2}} + \dots, \quad (\text{A1})$$

providing $\phi(0) = 0$. Here it will be shown that the index m must be 2 in order to have a physically meaningful value for the slow ion density on axis.

As before, attention is restricted to a small

region around the axis so that only the first term in Eq. (A1) is dominant. The integral in Eq. (2) becomes on simplification

$$n_i(a) = \frac{n_{b0} \sigma n v_b r_0}{(2e/m_i)^{1/2} (-\phi_0)^{1/2}} \int_0^1 \frac{u^{-(m-2)/m}}{m(1-u)^{1/2}} du,$$

where $u = r^m/a^m$. This integral may be solved to give

$$n_i(a) = \frac{n_{b0} \sigma n v_b r_0^{1-m/2}}{(2e/m_i)^{1/2} \phi_0^{1/2}} \sqrt{\pi} \frac{\Gamma[1 - (m-2)/m]}{\Gamma[\frac{3}{2} - (m-2)/m]}. \quad (\text{A2})$$

It can be seen that if m is greater than 2 when a tends to zero, the axial ion density tends to infinity. If m is less than 2, the axial ion density tends to zero. Both of these solutions are non-physical hence m must be exactly equal to 2 to yield a nonzero finite value for n_{i0} and this has been assumed in Eq. (3). Thus when $m=2$

$$n_{i0} = n_{b0} \sigma n v_b r_0 / (2e/m_i)^{1/2} \phi_0^{1/2}.$$

APPENDIX B: DISTRIBUTION OF NEWLY CREATED ELECTRONS

When electrons have been created by ionization, the beam ions give them a small amount of kinetic energy. A theoretical model by Gryzinski¹⁸ has determined this velocity distribution which is proportional to the beam velocity, v_b . Experimental work by Rudd and Jorgensen¹¹ has confirmed this velocity distribution. It is assumed here that this velocity is isotropic and hence the electrons will have an angular momentum of the order of ρw about the beam axis, where ρ is the radius at which they were created. This forces the electrons to have elliptic orbits around the beam axis if the potential well is parabolic. The equations of motion for the electrons are

$$\frac{1}{2} m_e v_r^2 + \frac{1}{2} m_e v_\theta^2 = e \Delta \phi + \frac{1}{2} m_e w^2$$

and

$$r v_\theta = \rho w,$$

where v_r and v_θ are the radial and azimuthal velocities and w is the initial velocity of the electron. If the well is assumed to be parabolic in the axial region then

$$\Delta \phi = (\phi_0/r_0^2)(\rho^2 - r^2)$$

Hence

$$\begin{aligned} v_r^2 &= (2e_0/m_e r_0^2)(\rho^2 - r^2) + w^2 - v^2 \\ &= (\rho^2 - r^2)[(2e\phi_0/m_e r_0^2)(w^2/r^2)]. \end{aligned}$$

The elliptical orbit intersects any given radius r , which is less than ρ , four times during a single orbit whose period τ is equal to $2(m_e r_0^2/2e\phi_0)^{1/2}$. Hence

$$\begin{aligned} \frac{dN_e}{dt} &= \int_r^\infty n n_b \sigma_i v_b \frac{4}{2\pi r v_r \tau} 2\pi \rho d\rho \\ &= \int_r^\infty n n_b e^{-\rho^2/r_0^2} \sigma_i v_b \\ &\quad \times \frac{4(2e\phi_0)^{1/2} \rho d\rho}{2\pi r (\rho^2 - r^2)^{1/2} (m_e r_0^2)^{1/2}} \\ &\quad \times \int_0^{w_m} \frac{f(w) dw}{(2e\phi_0/m_e r_0^2 - w^2/r^2)^{1/2}}, \end{aligned}$$

where $f(w)$ is the distribution function of the initial velocities and w_m^2 equals $2er^2\phi_0/m_e r_0^2$. This function may be approximated by

$$f(w) \approx (2/v_b^2) e^{-w^2/v_b^2} w dw.$$

This expression gives moderate agreement with

the results obtained by Rudd and Jorgensen except at low values of w .

If the above two equations are combined and $2e\phi_0 r^2/m_e r_0^2 v_b^2$ is less than unity which applies for $r < r_0$, then

$$\frac{dN_e}{dt} = \frac{4n n_b \sigma_i v_b r}{\pi^{1/2} r_0} \frac{e\phi_0}{m_e v_b^2}.$$

The net effect of the finite velocity of the electrons is to transfer the electrons from the center to edge as their angular momentum prevents most of these electrons from reaching the center of the beam. The above relation breaks down at radii greater than r_0 , but as the most effective energy absorption occurs at the center where the containment time is longest, this effect is unimportant.

- ¹J. G. Cordey, Proceedings on Theoretical and Experimental Aspects of Heating Toroidal Plasmas, Grenoble, 1976 (unpublished), Vol. 2, pp. 107-115.
²J. G. Cordey and W. G. F. Core, Nucl. Fusion **15**, 710 (1975).
³R. M. Kulsrad and D. L. Jassby, Nature **259**, 541 (1976).
⁴M. D. Gabovich, L. P. Katsubo, and I. A. Solovhenko, Sov. J. Plasma Phys., **1**, 16 2 (1975).
⁵G. Hamilton (private communication).
⁶D. A. Dunn and S. A. Self, J. Appl. Phys. **35**, 113 (1964).
⁷T. S. Green (unpublished).
⁸L. Spitzer, *Physics of Fully Ionized Gases* (Interscience, New York, 1962).
⁹J. G. Cordey, Phys. Fluids **14**, 1407 (1971).
¹⁰M. N. Rosenbluth, W. M. MacDonald, and D. L. Judd, Phys. Rev. **107**, 1 (1957).

- ¹¹M. E. Rudd and T. Jorgensen, Jr., Phys. Rev. **131**, 666 (1963).
¹²E. R. Harrison and W. B. Thompson, Proc. Phys. Soc. Lond. **74**, 145 (1959).
¹³A. J. T. Holmes and E. Thompson (unpublished).
¹⁴E. Thompson, Proceedings of the Conference on Ion Sources and Beams, Berkeley, 1974 (unpublished), Vol. II, p. 7.
¹⁵E. S. Solov'ev, R. N. Il'in, V. Oparin, and N. Fedorenko, Sov. Phys. JETP **18**, 342 (1964).
¹⁶S. K. Allison, Rev. Mod. Phys. **30**, 1137 (1958).
¹⁷I. Kapchinskij and V. Vladimirskij, *Proceedings of the High Energy Acceleration Conference* (CERN, Geneva, 1959), p. 274.
¹⁸E. S. Solov'ev, R. N. Il'in, V. Oparin, and N. Fedorenko, Sov. Phys. JETP **18**, 342 (1964).